Modelling with finite difference approximations to the wave-equation

John C. Bancroft

ABSTRACT

Analyzing waves on a string is informative relative to the properties of various solutions to the wave-equation, and to the parameters used in finite difference approximations to those solutions. In addition, insight may be gained to various problems such as estimating the reflection coefficients from the cross-correlation imaging conditions.

Solutions are compared between a constant velocity form and variable velocity form of the wave equations. The cross correlation imaging condition for various methods of wave-propagation is also evaluated.

INTRODUCTION

A basic solution to the wave equation assumes the velocity is constant, or relatively constant, over the span of a finite difference operator. It is often assumed, that if the space and time increments are small enough, then this solution will produce reasonable results, even in a medium with varying velocities. Modelling examples show that errors may occur in the amplitudes, and that polarities can be incorrect.

A slightly more complex solution allows the velocity to vary within the span of the operator. These solutions do provide the correct amplitudes and polarities of the transmitted and reflected energies.

The wave-equations and their solutions are evaluated on a 1D model, "string," that contains three areas with different velocities. Modelling shows the primary reflections, along with surface and interbed multiples.

THEORY

Wave equations

The wave-equation for the constant velocity is

$$\frac{\partial^2 P}{\partial t^2} = V^2 \frac{\partial^2 P}{\partial z^2}, \tag{1}$$

where P is the displacement, and V the velocity. The variable velocity equation is

$$\frac{\partial^2 P}{\partial t^2} = \frac{\partial}{\partial z}\left(V^2 \frac{\partial P}{\partial z} \right). \tag{2}$$

This equation may also be written as

$$\frac{\partial^2 P}{\partial t^2} = V^2 \frac{\partial^2 P}{\partial z^2} + \frac{\partial Z^2}{\partial z}\frac{\partial P}{\partial z}, \tag{3}$$

where the portion in blue indicates an additional term that is not present in the constant velocity solution. This reduces to a usable form

$$\frac{\partial^2 P}{\partial t^2} = V^2 \frac{\partial^2 P}{\partial z^2} + 2V \frac{\partial Z}{\partial z}\frac{\partial P}{\partial z}. \tag{4}$$

Finite difference solutions for the first and second derivatives

First derivative approximations

These equations are solved using finite difference approximations for the first and second derivative. The first derivative will be approximated with three possibilities; with the first a poor choice as it introduces phase errors. The second three-point approximation, where $P(z) = 0$, is more common, but it not as accurate as the seven point solution in equation (7).

$$\frac{dP}{dx} \approx \frac{P(z+\delta z) - P(z)}{\delta z}, \tag{5}$$

$$\frac{dP}{dx} \approx \frac{P(z+\delta z) - P(z-\delta z)}{2\delta z}, \tag{6}$$

and

$$\frac{dP_0}{dx} \approx \frac{-P_{-3} + 9P_{-2} - 45P_{-1} + 45P_1 - 9P_2 + P_3}{60\delta x}, \tag{7}$$

where in equation (7) now contains subscripts to identify the preceding and following samples.

Second derivative approximations

The second derivative is approximated with the tree point solution

$$\frac{d^2 P_0}{dx^2} \approx \frac{P_{-1} - 2P_0 + P_1}{\delta x^2}, \tag{8}$$

with a seven-point solution

$$\frac{d^2 P_0}{dx^2} \approx \frac{2P_{-3} - 27P_{-2} + 270P_{-1} - 490P_0 + 270P_1 - 27P_2 + 2P_3}{60\delta x^2}. \tag{9}$$

Higher and lower order solution are available for the first and second derivatives, along with solutions that are not centrally organized at P_0.

Finite difference solutions to the wave equations

Constant velocity three point solution

Using the three point solution for the second derivative, where the "*i*" subscript is for displacement, and the "*j*" subscript for time their finite difference equation becomes,

$$\frac{P_{j-1}-2P_j+P_{j+1}}{\delta t^2}=V^2\frac{P_{i-1}-2P_i+P_{i+1}}{\delta z^2}, \tag{10}$$

and solving for the new time sample we have

$$P_{j+1}=2P_j-P_{j-1}+\frac{V^2\delta t^2}{\delta z^2}\left(P_{i-1}-2P_i+P_{i+1}\right). \tag{11}$$

The variable velocity three point solution

The variable velocity finite difference equation is

$$\frac{P_{j-1}-2P_j+P_{j+1}}{\delta t^2}=V_0^2\frac{P_{i-1}-2P_i+P_{i+1}}{\delta z^2}+2V_i\frac{V_{i+1}-V_{i-1}}{2\delta z}\frac{P_{i+1}-P_{i-1}}{2\delta z}, \tag{12}$$

and solving for the new time sample

$$P_{j+1}=2P_j-P_{j-1}+\frac{V_0^2\delta t^2}{\delta z^2}\left(P_{i-1}-2P_i+P_{i+1}\right)+\frac{\delta t^2}{4\delta z^2}\left(V_{i+1}^2-V_{i-1}^2\right)\left(P_{i+1}-P_{i-1}\right). \tag{13}$$

We can also solve for a new depth sample

$$P_{i+1}=\left[2P_i-P_{i-1}\frac{\delta z^2}{V_0^2\delta t^2}\left(P_{j-1}-2P_j+P_{j+1}\right)+\frac{V_{i+1}^2-V_{i-1}^2}{4V_0^2}P_{i-1}\right]\left(1+\frac{V_{i+1}^2-V_{i-1}^2}{4V_0^2}\right)^{-1}. \tag{14}$$

In time stepping, the ratio $\frac{V_0^2\delta t^2}{\delta z^2}$ must be less than unity for stability.

In depth stepping the ratio $\frac{\delta z^2}{V_0^2\delta t^2}$ must be less than unity and is the inverse of that required for time stepping. Consequently, different grid sizes are required if stepping in time or in displacement.

The seven point solutions are not shown.

Reflection and transmission coefficients for 1D model

The transmission coefficient is

$$T_{1-2}=\frac{2Z_1}{Z_1+Z_2}\ . \tag{15}$$

The reflection coefficient for a string is

$$R_{1-2} = \frac{Z_1 - Z_2}{Z_1 + Z_2} \ . \qquad (16)$$

MODEL

A 1D model of a string was chosen for modelling as it is possible to view the motion in a 3D perspective plot showing the displacement, time, and amplitude. It represents a vertical 1D trace.

The string is composed of three sections with velocities of 1,000, 2,000, and 900 m/s, with the top at z = 0, being totally reflective, and the bottom at z = 200 m. being totally absorptive. The transmission coefficient for the first interface is 0.6666, and the reflection coefficient is -0.3333, (i.e. negative). Energy is inserted with a wavelet at depth z = 0, and a second wavelet at $z = 0 + \delta z$. The transition zone has a cosine shape that is spread over 21 depth samples. The following tests were conducted with a time sample interval of 0.0000625 sec, and a depth increment of 0.125 m.

Fig. 1 shows the initial wavelets for initializing the process at times, 0.00000 and 0.0000625 sec, and also at time t = 0.050 sec, when the wavelet has passed the first boundary identified by the blue "+" sign. The variable velocity wave equation was used, and the amplitudes of transmitted and reflected wavelets are correct. If the process was run using a larger time sample increment of 0.000125 sec., the width and amplitude of the reflected wavelet showed visible distortion. The accuracy of the amplitudes of the transmitted and reflected wavelets for various sampling rates is presented in the Appendix.

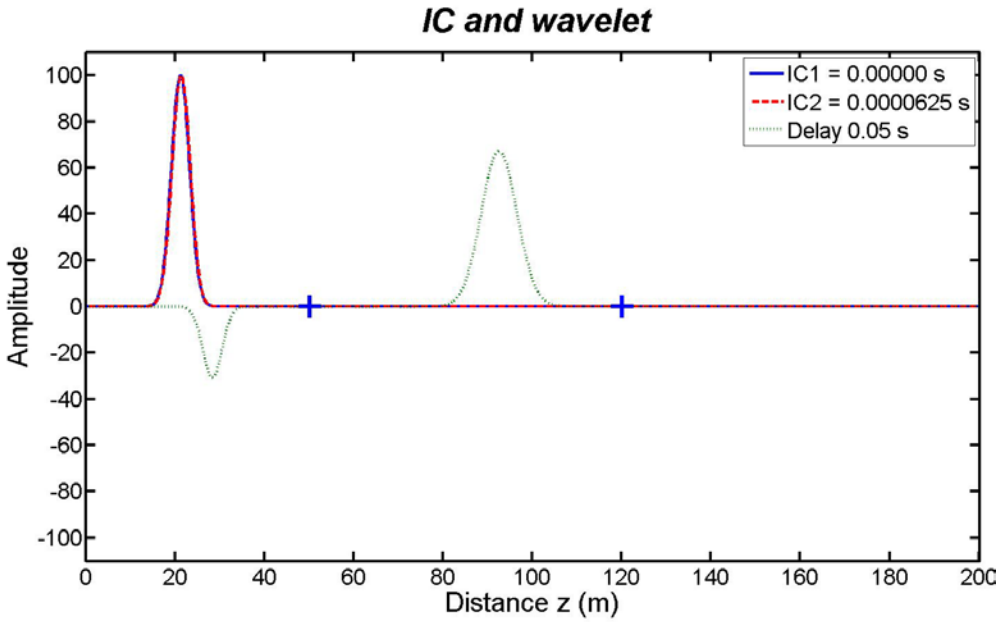

Fig. 1: Wavelets at initial time and at time 0.050 sec. showing the incident amplitude, the reflected amplitude in green at depth 25 m, and the transmitted amplitude at 90 m.

A two dimensional perspective view of the wave propagation is displayed in Fig. 2 using the constant velocity wave-equation. The kinematics are accurate, and the down-going incident, primary reflections, and multiple reflection wavelets are visible and look correct. However, after the first velocity transition, the amplitude of the transmitted wave is greater than 1.0, (it should be 0.666 s), and the first reflection has the wrong polarity (it should be negative).

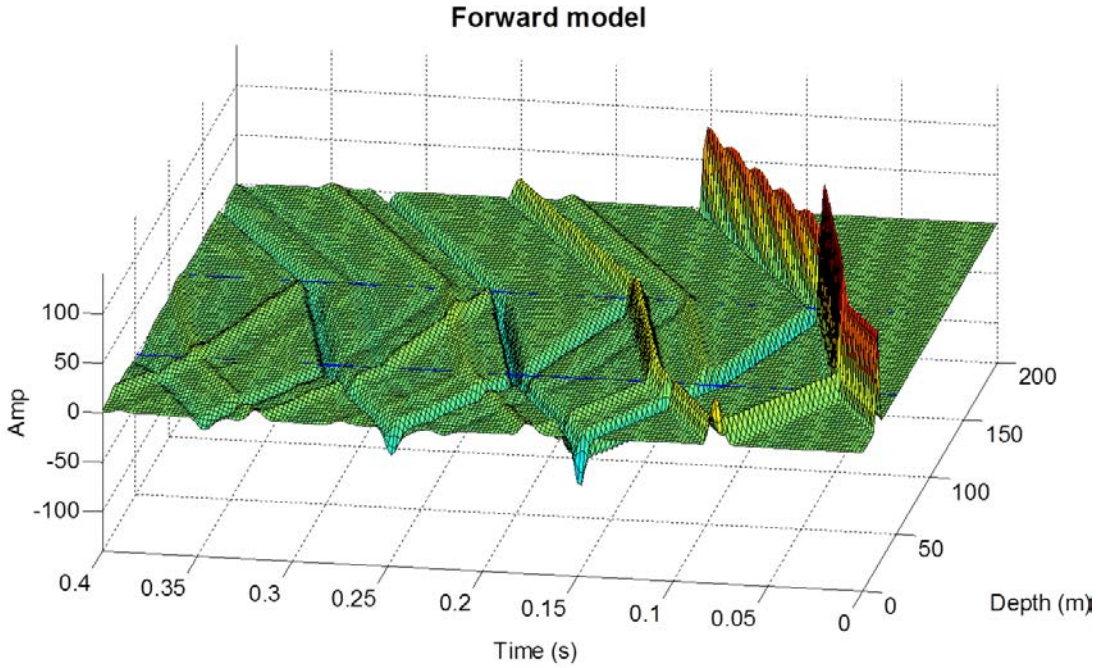

Fig. 2: Forward model using the constant velocity wave equation displaying errors.

The variable velocity solution is shown in Fig. 3, where the transmitted amplitude is now correct, and the reflection has the correct polarity.

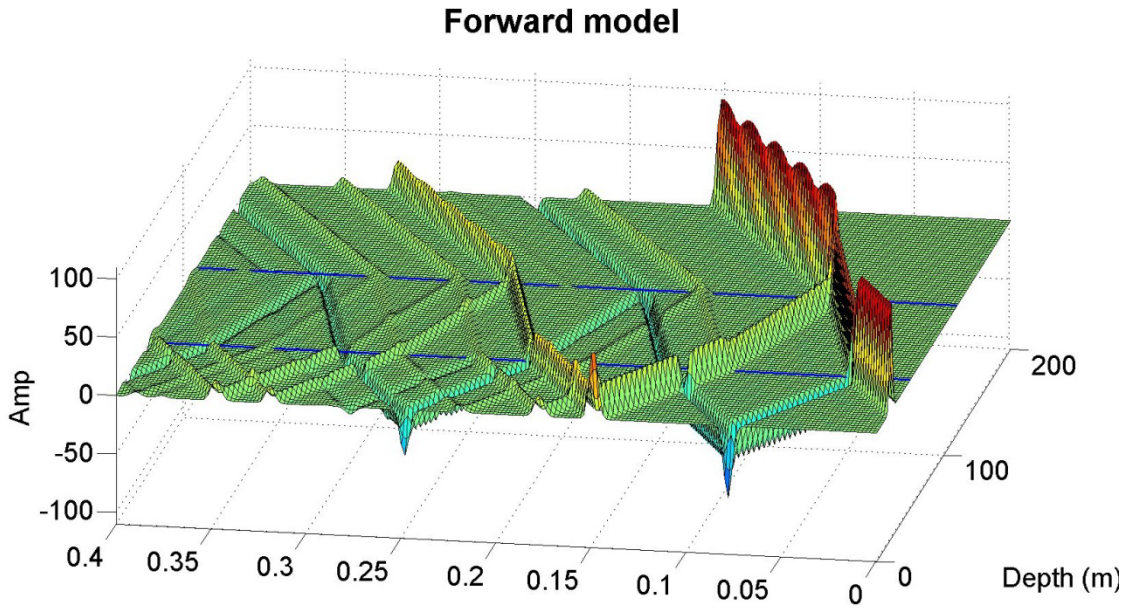

Fig. 3: Correct forward model using the variable velocity wave equation.

Reconstructing the model

The data in the forward model can be recreated using either a reverse time or a downward continuation process. These complete reconstructions require data at the three boundaries $z = 0$, $z = z_{max}$. and $t = t_{max}$. When considering surface seismic, only data at z = 0 is available. Reconstruction of the wavefield will not be complete. The following figure shows reconstructions with reverse time using the same finite difference solution as the forward model.

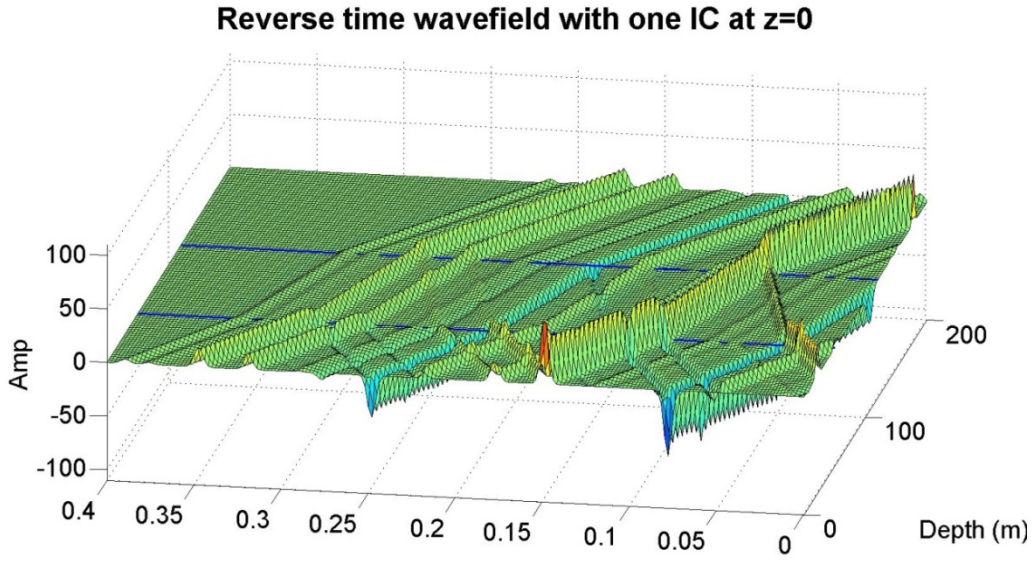

Fig. 4 Reconstruction of the wavefield using reverse time.

Fig. 5 show the wavefield reconstruction using a one-way downward continuation phaseshift algorithm.

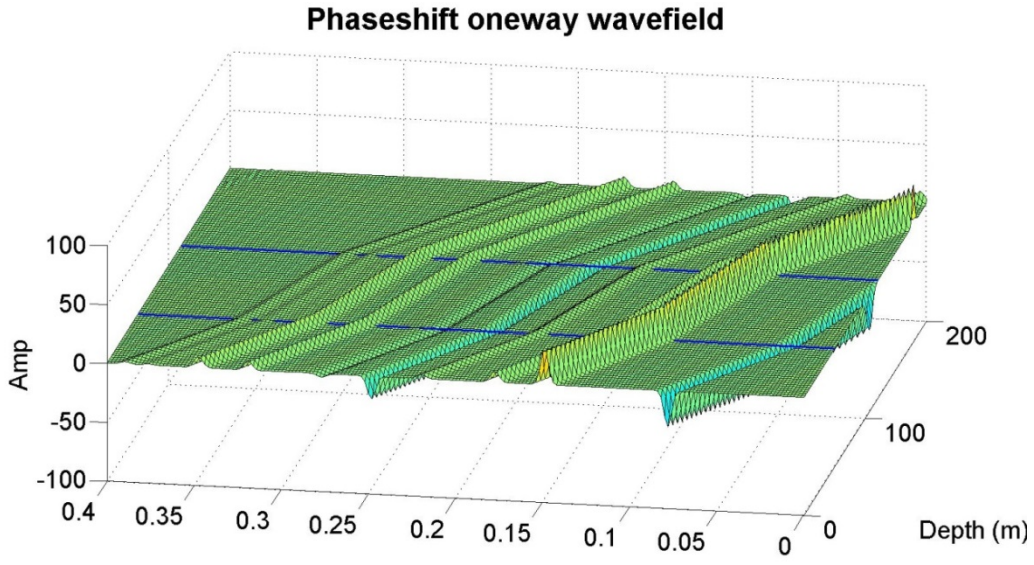

Fig. 5: Reconstruction using a phase shift algorithm with primaries and multiples.

If we assume the multiples have been removed, then phase-shift algorithm will produce the back projected primaries as in Fig. 6.

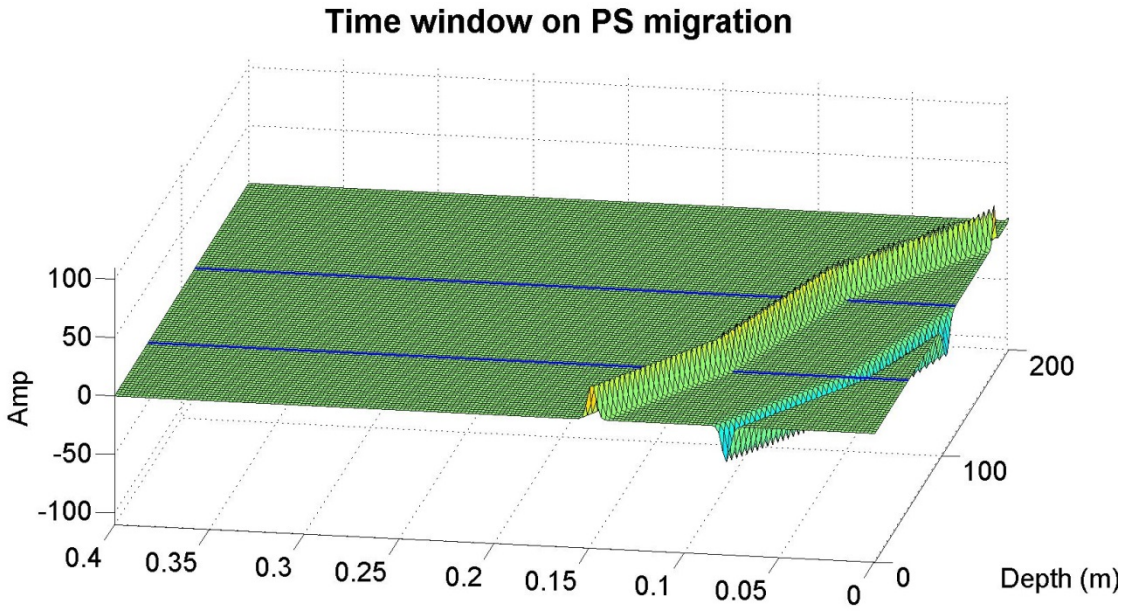

Fig. 6: Phaseshift reconstruction of the primaries.

The downward propagating energy of the forward model is simulated with a window as illustrated in Fig. 7. A cross correlation with the phase shift primaries produces the result in Fig. 8, that is similar to the reflectivity.

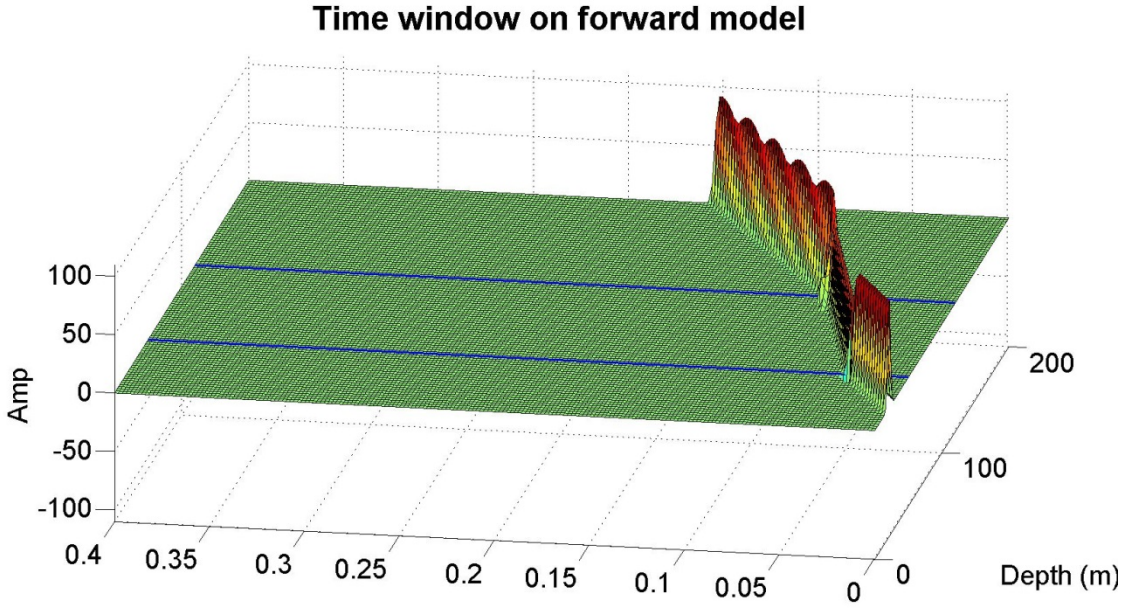

Fig. 7 Window passing the forward modelled primaries.

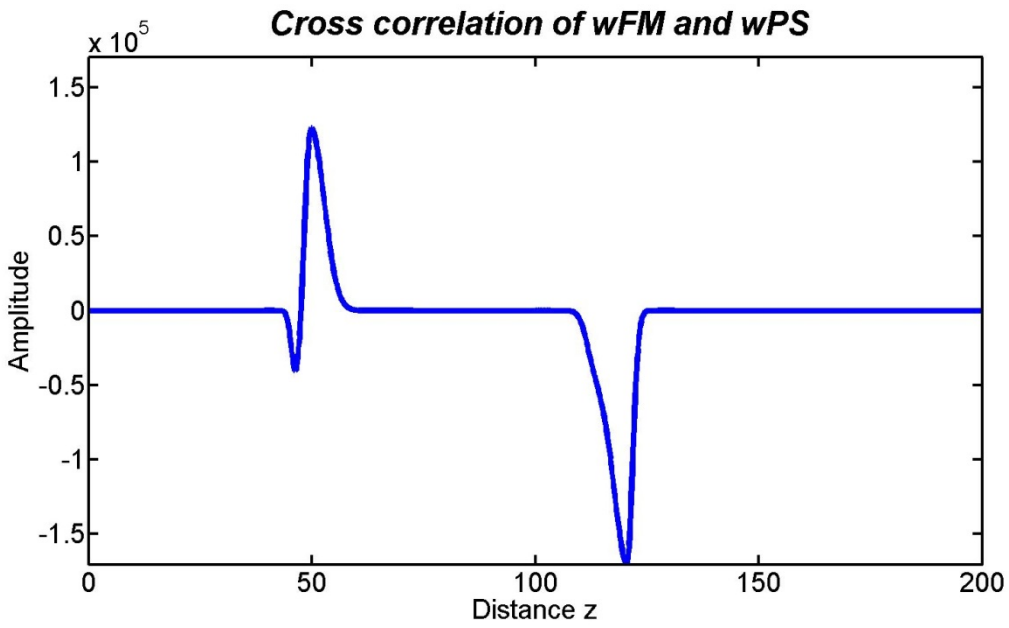

Fig. 8: Cross correlation of the phaseshift primaries with the windowed forward model.

COMMENTS AND CONCLUSIONS

There is a significant error when using a constant velocity wave-equation to model data in a medium with slowly varying velocities. These errors can be changes in the amplitudes of the transmitted and reflected energies. The polarity of the reflection may also be in error.

A multiple free reconstruction of the wavefield using a phaseshift algorithm with a windowed forward model containing the incident wavelets produces a cross-correlation that matches the amplitudes of the reflectivities without low frequency noise.

ACKNOWLEDGEMENTS

We thank the sponsors of CREWES for their support. We also gratefully acknowledge support from NSERC (Natural Science and Engineering Research Council of Canada) through the grant CRDPJ 379744-08.

APPENDIX

The sample intervals for time and depth were selected from the following cases.

```
case 3;     Dz     = 0.500;     Dt     = 0.00025;
case 4;     Dz     = 0.250;     Dt     = 0.000125;
case 5;     Dz     = 0.125;     Dt     = 0.0000625;
case 6;     Dz     = 0.0625;    Dt     = 0.00003125;
case 7;     Dz     = 0.03125;   Dt     = 0.000015625;
```

The peak of the transmitted and reflected wavelets were:

Case 3 Trans. = 0.688, Refl. = -0.160
Case 4 Trans. = 0.671, Refl. = -0.309
Case 5 Trans. = 0.671, Refl. = -0.309
Case 6 Trans. = 0.667, Refl. = -0.327
Case 7 Trans. = 0.666, Refl. = -0.333

The plots for cases 3 and 4 are shown below in Fig. 9 and Fig. 10.

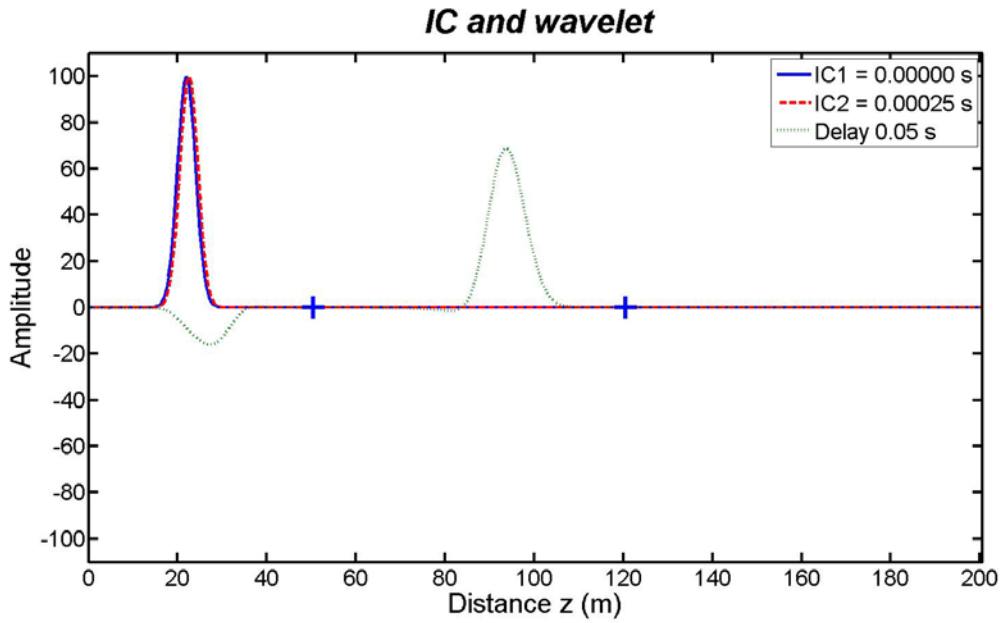

Fig. 9: Wavelets for case 3.

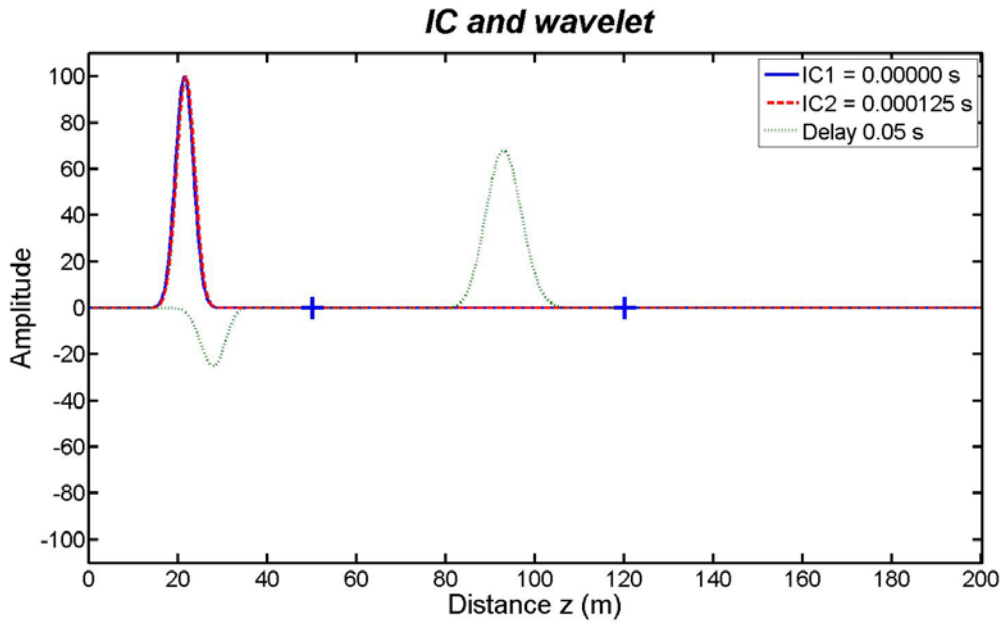

Fig. 10: Wavelets for case 4.